

Estimations of phonon-induced decoherence in silicon–germanium triple quantum dots

Alexander Yu. Vasiliev · Leonid Fedichkin

Received: 4 March 2014 / Accepted: 13 June 2014 / Published online: 26 June 2014
© Springer Science+Business Media New York 2014

Abstract The decoherence and dephasing rate of charge qubits in systems based on double and triple SiGe quantum dots are studied. At the short time limit, electron–phonon interaction causes an incomplete decay of the off-diagonal density matrix elements. Long-time relaxation decay dominates over dephasing at large times. The triple quantum dot system with the same interdot distance demonstrates lower relaxation rate in the wide range of parameters.

Keywords Quantum computation · Nanotechnology · Quantum dots · Phonons · Charge qubit · Decoherence

1 Introduction

For the last years, semiconductor quantum dots are considered to be one of the most realistic nanodevices for the quantum information processing. Recent experiments [1] have shown that coherent quantum oscillations of singlet-triplet spin qubits in Si/SiGe have longer intrinsic spin coherent times than singlet-triplet qubits in GaAs. The control over spin states has made remarkable progress; however, spin qubits demonstrate

A. Yu. Vasiliev · L. Fedichkin
NIX, 19, Zvezdny blvd, 129085 Moscow, Russia

L. Fedichkin
Institute of Physics and Technology, Russian Academy of Sciences,
34 Nahimovskii pr., 117218 Moscow, Russia

A. Yu. Vasiliev · L. Fedichkin (✉)
Dept. of Theoretical Physics, Moscow Institute of Physics and Technology,
9 Institutsky per., Dolgoprudny, Moscow Region 141700, Russia
e-mail: leonid@phystech.edu; leonidf@gmail.com

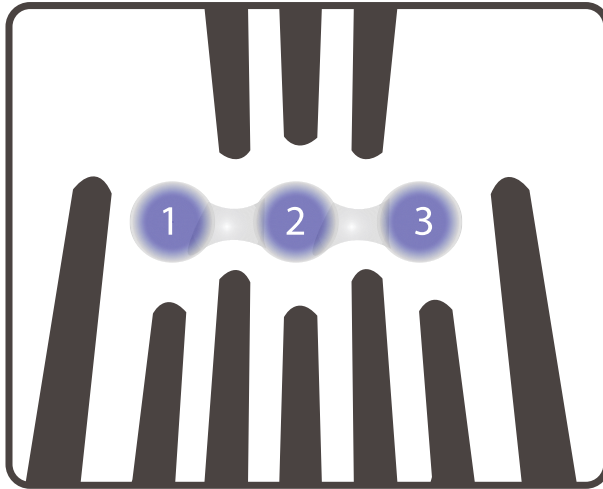


Fig. 1 The sketch of the triple quantum dot system and its control electrodes

substantial decoherence still. Due to mixing of electron spin degrees of freedom with spatial (charge) degrees, one has to look for the methods to extend spatial coherence. This work investigates the above-mentioned experimental results and related alternative scheme.

It is important to examine how electron–phonon interaction can affect the coherent oscillations, because it is inherent to semiconductor nanostructures. In this work, we analyze decoherence of single electron in a double and triple dot potentials due to electron interaction with acoustic phonons. These structures can be fabricated as gate-engineered quantum dots, whose potential distribution is determined by the external metallic top-gates. Firstly, we consider a single electron in the double well potential with anisotropic electron–phonon coupling, examining the relaxation and phase damping rate. Furthermore, we consider triple quantum dot confining one electron and find the parameter’s spacing where this system would have advantages over conventional double dot. The schematic representation of triple quantum dot is shown in Fig. 1. This system as a basis for quantum bit implementation has attracted attention recently [2,3].

2 The properties of structure

For definiteness, we will focus our consideration on properties of experimental Si/SiGe quantum dot structure recently studied in [1]. The electron–phonon interaction in thin Si layer differs from electron–phonon interaction in bulk Si because of strain effect. In our case, the layer containing two-dimensional electron gas is a strained silicon quantum well, lying on buffer of $\text{Si}_{0.71}\text{Ge}_{0.29}$ [4]. Lattice deformation leads to band structure change. Since lattice constants of heterolayers are mismatched $l_1/l_0 = 1.0094$, Si layer is squeezed along [001] direction perpendicular to heterointerface. Poisson constant of Si $\mu = 0.266$; therefore, silicon is squeezed in accordance with

$\varepsilon_z = \mu(l_1 - l_0)/l_0 = -0.0025$. This deformation decreases in effect the gap for [100] and [010] by 0.0375 eV and increases gap for [001] by 0.0125 eV [5]. Therefore, at temperatures below 1 K, the influence of upper valley is neglected.

The electron–phonon interaction can be expressed as

$$\begin{aligned}
 H_{ep} = & \mathcal{E}_d \Sigma \left(\frac{\hbar}{2\rho_s q V} \right)^{1/2} |q| P(\bar{q}) \left(b_{\bar{q}} + b_{\bar{q}}^{\dagger} \right) \\
 & + \mathcal{E}_u \sum_{\alpha} (\bar{k}_{\alpha} \bar{q})^2 \left(\frac{\hbar}{2\rho_s q V} \right)^{1/2} |q|^{-1} P(\bar{q}) \left(b_{\bar{q}} + b_{\bar{q}}^{\dagger} \right) \tag{1}
 \end{aligned}$$

Here, $b_{\bar{q}}, b_{\bar{q}}^{\dagger}$ — phonon annihilation/creation operators, $P(\bar{q})$ —the formfactor of triple quantum dot, \bar{q} — phonon wave vector, $P(\bar{q})$ —formfactor. \bar{k}_{α} are directed toward [010] and [100] valleys, respectively. Following Ref. [5], we use the following values for material constants $\mathcal{E}_u = 10.5$ eV, $\mathcal{E}_d = 3.34$ eV.

Quantum dots are shaped by the repulsive potential of top metal gates. Following [6], we take an appropriate wave-function for quantum well. The electron wavefunction at the heterointerface is relatively thin in perpendicular direction with characteristic size of about 3 nm. The size of quantum dot in lateral directions can be few tens of nm depending on structure geometry and potential at the gates. For large quantum dots with diameter more than 50 nm, the distance between energy levels goes below temperature range of 100 mK that prevents experimental observation of quantum coherent effects. The electron wavefunction for triple quantum dot system is taken in the form

$$\Psi_i(\bar{q}) = \frac{1}{a_2^{1/2} a_1 \pi^{3/4}} e^{-\frac{1}{2} a_1^2 (q_y^2 + q_x^2) - \frac{1}{2} a_2^2 q_z^2} e^{-i\bar{q}\bar{R}_i} \tag{2}$$

Here, $a_1 = 47$ nm, $a_2 = 3$ nm, \bar{R}_i is the vector corresponding to the centers of $i = (1, 2, 3)$ quantum dots

Hence, the formfactor is

$$P(\bar{q}) = \frac{1}{a_2 a_1^2 \pi^{3/2}} e^{-a_1^2 (q_y^2 + q_x^2) - a_2^2 q_z^2} e^{-i\bar{q}\bar{R}} \sum_i e^{-i\bar{q}\bar{R}_i} c_i^{\dagger} c_i \tag{3}$$

3 Decoherence in triple quantum dot system

3.1 Phase damping

To investigate decoherence dynamic at small times, we have to consider evolution of entanglement between quantum system of interest and environment. In our case, single electron in triple quantum dot interacts with phonon reservoir. The temporal behavior is governed by the Hamiltonian

$$H = H_0 + H_{ep} + \sum_{\bar{q}} b_{\bar{q}}^{\dagger} b_{\bar{q}} \omega_{\bar{q}} \tag{4}$$

Here:

$$H_0 = \begin{pmatrix} \varepsilon_1 & 0 & 0 \\ 0 & \varepsilon_2 & 0 \\ 0 & 0 & \varepsilon_3 \end{pmatrix} \tag{5}$$

The electron–phonon hamiltonian can be represented in this way:

$$H_{ep} = \sum_i Q_i F_i \tag{6}$$

$$Q_i = c_i^+ c_i \tag{7}$$

Here, the operators F_i are referred to the reservoir and operators Q_i act on system’s variables.

To study phase decoherence effects, we chose intentionally the realistic situation of qubit operation as memory cell when interdot barriers are high so that electron tunneling is suppressed. Then, electron–phonon interaction term in our Hamiltonian commutes with electron term; therefore, there is no energy exchange between electron and phonon reservoir. To calculate the rate of phase damping, we should split the formfactor in electron–phonon hamiltonian on nontrivial and identity terms

$$\begin{aligned} P(\bar{q}) &= \frac{1}{a_2 a_1^2 \pi^{3/2}} e^{-a_1^2(q_y^2 + q_x^2) - a_2^2 q_z^2} e^{-i\bar{q}\bar{R}} \sum_i e^{-i\bar{q}\bar{R}_i} c_i^+ c_i \\ &= \frac{1}{a_2 a_1^2 \pi^{3/2}} e^{-a_1^2(q_y^2 + q_x^2) - a_2^2 q_z^2} e^{-i\bar{q}\bar{R}} \\ &\quad \times (A (c_1^+ c_1 + c_2^+ c_2 + c_3^+ c_3) + B (c_1^+ c_1 - c_2^+ c_2) + C (c_2^+ c_2 - c_3^+ c_3)) \end{aligned} \tag{8}$$

The two latter terms give rise to electron dephasing.

The evolution operator [7] is as follows:

$$\begin{aligned} U(t) &= \exp \left\{ -i \int_0^t \sum_q (B\sigma_z^{12} + C\sigma_z^{23}) (g_q b_q^+ e^{i\omega_q t'} + g_q^* b_q e^{-i\omega_q t'}) dt' \right\} \\ &= \exp \left\{ (B\sigma_z^{12} + C\sigma_z^{23}) \frac{1}{2} \sum_q (b_q^* \xi_q(t) - b_q \xi_q^*(t)) \right\} \end{aligned} \tag{9}$$

Here,

$$\xi_q(t) = 2g_q \frac{1 - e^{i\omega_q t}}{\omega_q} \tag{10}$$

$$g_q = \left(\frac{\hbar}{2\rho s q V} \right)^{1/2} \left(\Xi_d |q| + \Xi_u |q|^{-1} \sum_{\alpha=1,2} (\bar{k}_\alpha \bar{q})^2 \right) e^{-a^2(q_y^2 + q_x^2) - a_z^2 q_z^2} \tag{11}$$

The states are transformed by evolution operator into the following:

$$\begin{aligned} & (c_1 |1\rangle + c_2 |2\rangle + c_3 |3\rangle) \otimes |0_q\rangle \xrightarrow{U(t)} \\ & \rightarrow c_1 |1\rangle \left| \frac{1}{2} \xi_q(t) B \right\rangle + c_2 |2\rangle \left| \frac{1}{2} \xi_q(t) (C - B) \right\rangle + c_3 |3\rangle \left| -\frac{1}{2} \xi_q(t) C \right\rangle \end{aligned} \tag{12}$$

Reduced density matrix elements are as follows:

$$\rho_{ij}(t) = \langle i | \text{Tr}_R U(t) \zeta(0) U^{-1}(t) | j \rangle \tag{13}$$

The diagonal elements of density matrix remain constant [7]. For example, element ρ_{11} :

$$U^{-1}(t) |1\rangle \otimes \psi = |1\rangle \otimes \prod_q D \left(\frac{1}{2} \xi_q(t) B \right) |\psi_q\rangle \tag{14}$$

$$\begin{aligned} \rho_{11}(t) &= \langle 1 | \text{Tr}_R U(t) \zeta(0) U^{-1}(t) | 1 \rangle \\ &= \prod_q \text{Tr}_q \left\{ R_{qT} D \left(\frac{1}{2} \xi_q(t) B \right) D \left(-\frac{1}{2} \xi_q(t) B \right) \right\} \\ \rho_{11}(0) &= \prod_q \text{Tr}_q R_{qT} \rho_{11}(0) = \rho_{11}(0) \end{aligned} \tag{15}$$

While off-diagonal terms:

$$\begin{aligned} \rho_{12}(t) &= \langle 1 | \text{Tr}_R U(t) \zeta(0) U^{-1}(t) | 2 \rangle \\ &= \prod_q \text{Tr}_q \left\{ R_{qT} D \left(\frac{1}{2} \xi_q(t) B \right) D \left(\frac{1}{2} \xi_q(t) (C - B) \right) \right\} \rho_{12}(0) \\ &= \prod_q \text{Tr}_q \left\{ R_{qT} D \left(\frac{1}{2} \xi_q(t) C \right) \right\} \rho_{12}(0) = e^{-B_{12}^2(t)} \rho_{12}(0) \end{aligned} \tag{16}$$

Following [1]:

$$B_{12}^2(t) \propto \int dq |g_q C|^2 \coth \left(\frac{\omega_q}{2T} \right) \frac{1 - \cos \omega_q t}{\omega_q} \tag{17}$$

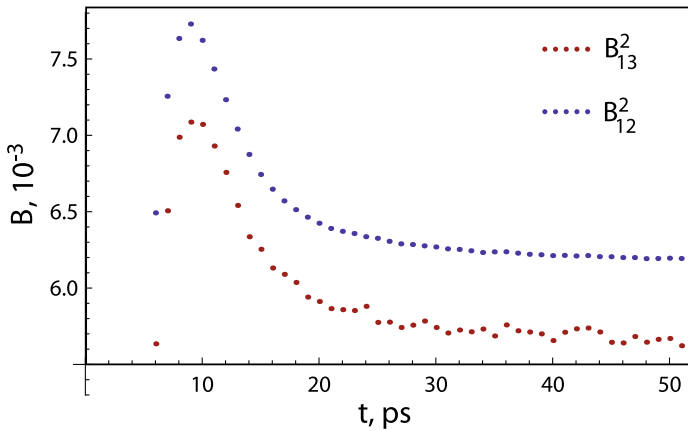


Fig. 2 The time dependence of spectral function for B_{12} and B_{13} nondiagonal elements

Compare the values of spectral function for different off-diagonal elements

$$B_{12}^2 = \frac{V}{\hbar^2 \pi^3} \int d^3q \frac{|g_q C|^2}{q^2 s^2} \coth\left(\frac{\hbar q s}{2k_B T}\right) \sin^2\left(\frac{q s t}{2}\right) \tag{18}$$

$$B_{13}^2 = \frac{V}{\hbar^2 \pi^3} \int d^3q \frac{|g_q(B-C)|^2}{q^2 s^2} \coth\left(\frac{\hbar q s}{2k_B T}\right) \sin^2\left(\frac{q s t}{2}\right) \tag{19}$$

$$B_{23}^2 = \frac{V}{\hbar^2 \pi^3} \int d^3q \frac{|g_q B|^2}{q^2 s^2} \coth\left(\frac{\hbar q s}{2k_B T}\right) \sin^2\left(\frac{q s t}{2}\right) \tag{20}$$

The expression for spectral function B_{12}^2 is similar to expression for the case of double dot system:

The maximum value of B_{12}^2 reaches $7.8 \cdot 10^{-3}$ at 8 ps. Asymptotic value of B_{12}^2 at large times is $6.2 \cdot 10^{-3}$ (Fig. 2).

Values of spectral function B_{23}^2 are lower than values of B_{12}^2 ; therefore, the decoherence at small times will be dominated by spectral function B_{12}^2 .

3.2 Relaxation

Consider the case of asymmetrical potential distribution in triple quantum dot system. The corresponding Hamiltonian

$$H_0 = \begin{pmatrix} \varepsilon_P & \varepsilon_A & 0 \\ \varepsilon_A & 0 & \varepsilon_A \\ 0 & \varepsilon_A & -\varepsilon_P \end{pmatrix} \tag{21}$$

One must take into account the relaxation decoherence effect in the three-level system, because electron–phonon interaction term does not commute with initial hamiltonian. In the condition of low temperatures, we are interested in low energy oscilla-

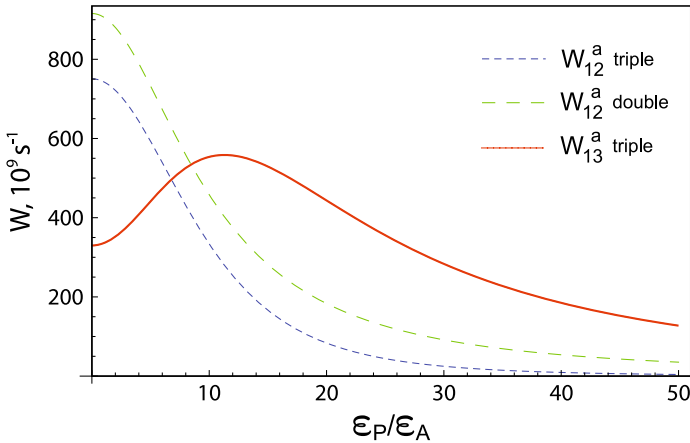


Fig. 3 The absorption probabilities for double and triple quantum dot systems

tion between states with eigenvalues equal $-\sqrt{\epsilon_P^2 + 2\epsilon_A^2}$ and 0. The probability for the absorption of the phonon due to excitation from the ground state to the upper level is [8]

$$W_{i \rightarrow f} = \frac{V}{(2\pi)^2 \hbar} \int d^3q |\langle f | H_{ep} | i \rangle|^2 \delta(\Delta\epsilon_{ij} - \hbar sq) \tag{22}$$

where $|i\rangle$ is the initial state with extra phonon with energy $\hbar sq$ and $|f\rangle$ is the final state, and q is the wave vector. The transitions to the lower energy state correspond to emission processes; in the other case, we have absorption processes. The parameter

$$a = \epsilon_P / \epsilon_A \tag{23}$$

accounts for localization of eigenstates in the centers of quantum dots. The dependence of absorption probabilities for transitions between states $|1\rangle - |2\rangle$ and $|1\rangle - |3\rangle$ from a is shown on Fig. 3 for comparison with double dot system. The time dependence for diagonal elements of density matrix is described with Liouville equation

$$\frac{d\rho_{11}}{dt} = (-W_{21}^a - W_{13}^a) \rho_{11} + W_{12}^c \rho_{22} + W_{31}^c \rho_{33} \tag{24}$$

$$\frac{d\rho_{22}}{dt} = W_{12}^a \rho_{11} + (-W_{12}^c - W_{12}^a) \rho_{22} + W_{12}^c \rho_{33} \tag{25}$$

$$\frac{d\rho_{33}}{dt} = W_{13}^a \rho_{11} + W_{12}^a \rho_{22} + (-W_{31}^c - W_{12}^c) \rho_{33} \tag{26}$$

which is simplified due to

$$W_{32}^c = W_{12}^c, \tag{27}$$

$$W_{32}^a = W_{12}^a. \tag{28}$$

The values of absorption probability for different cases versus $\mathbf{a} = \boldsymbol{\varepsilon} \mathbf{p} / \boldsymbol{\varepsilon}_A$:

3.3 Calculation of nondiagonal elements

Consider nondiagonal elements for Liouville equation. Following Ref. [9], we can split each coefficient onto independent parts

$$\langle m' | \dot{\rho}(t) | m \rangle = -\gamma_{m'm} \langle m' | \rho(t) | m \rangle \tag{29}$$

$$\gamma_{m'm} = \sum_k (\Gamma_{m'kkm'}^+ + \Gamma_{mkkm}^-) - \Gamma_{mmm'm'}^+ - \Gamma_{mmm'm'}^- \tag{30}$$

Where:

$$\Gamma_{mklm}^+ = (1/\hbar)^2 \sum_{ij} \langle m | Q_i | k \rangle \langle l | Q_j | n \rangle \int dt' \exp(-i\omega_{ln}t') \langle F(t')_i F_j \rangle \tag{31}$$

$$\Gamma_{mklm}^- = (1/\hbar)^2 \sum_{ij} \langle m | Q_j | k \rangle \langle l | Q_i | n \rangle \int dt' \exp(-i\omega_{mk}t') \langle F(t')_j F_i \rangle \tag{32}$$

$$\omega_{mn} = (E_m - E_n) / \hbar \tag{33}$$

In the case of one-phonon approximation, we have sums of Γ^- and Γ^+ terms with $\omega_{ln} = 0$ and same indexes equal zero. Consider the integrals in the right side of summands

$$\begin{aligned} \int_0^\infty dt' \exp(-i\omega_{mk}t') \langle F_j F(t')_i \rangle &= \int_0^\infty dt' \exp(-i\omega_{mk}t') \text{tr}_R [F(t')_i F_j \rho(0)_R] \\ &= \sum_{N'N} \langle N' | F_j | N \rangle \langle N | F_i | N' \rangle \langle N' | \rho(0)_R | N' \rangle \\ &\quad \times \int_0^\infty dt' \exp[i(E_{N'} - E_N - \hbar\omega_{mk})t'/\hbar] \end{aligned} \tag{34}$$

The indexes N and N' correspond to initial and final states of reservoir. Further

$$\begin{aligned} &\Gamma_{mklm}^+ + \Gamma_{mklm}^- \\ &= (1/\hbar)^2 \sum_{ijNN'} \langle m | Q_i | k \rangle \langle l | Q_j | n \rangle \langle N' | F_i | N \rangle \langle N | F_j | N' \rangle \langle N' | \rho(0)_R | N' \rangle \\ &\quad \times \int_0^\infty dt' \exp[i(E_{N'} - E_N - \hbar\omega_{ln})t'/\hbar] \end{aligned}$$

$$\begin{aligned}
 &+ (1/\hbar)^2 \sum_{ijNN'} \langle m | Q_j | k \rangle \langle l | Q_i | n \rangle \langle N' | F_j | N \rangle \langle N | F_i | N' \rangle \langle N' | \rho(0)_R | N' \rangle \\
 &\times \int_0^\infty dt' \exp[i (E_{N'} - E_N - \hbar\omega_{ln}) t' / \hbar] \\
 &= (1/\hbar)^2 \sum_{ijNN'} |\langle mN | V | nN' \rangle|^2 \langle N' | \rho(0)_R | N' \rangle \delta (E_{N'} - E_N - \hbar\omega_{ln}) \quad (35)
 \end{aligned}$$

In the case of

$$\omega_{ln} = 0 \quad (36)$$

we have

$$E_{N'} = E_N \quad (37)$$

which means that initial and final states are the same. In the case of one-phonon approximation, we have zero amplitude of transition between two levels with similar energy.

And finally, we can define each coefficient shortly

$$\gamma_{12} = \Gamma_{1221}^+ + \Gamma_{1331}^+ + \Gamma_{2112}^- + \Gamma_{2332}^- \quad (38)$$

$$\gamma_{13} = \Gamma_{1331}^+ + \Gamma_{1221}^+ + \Gamma_{3113}^- + \Gamma_{3223}^- \quad (39)$$

$$\gamma_{32} = \Gamma_{3113}^+ + \Gamma_{3223}^+ + \Gamma_{2112}^- + \Gamma_{2332}^- \quad (40)$$

We can express real and imaginary part of each coefficient

$$\begin{aligned}
 \Gamma_{mkl n}^+ &= (1/\hbar)^2 \sum_{ijNN'} \langle m | Q_i | k \rangle \langle l | Q_j | n \rangle \langle N' | F_i | N \rangle \langle N | F_j | N' \rangle \langle N' | \rho(0)_R | N' \rangle \\
 &\times \int_0^\infty dt' \exp[i (E_{N'} - E_N - \hbar\omega_{ln}) t' / \hbar] \\
 &= (1/\hbar)^2 \sum_{ijNN'} \langle m | Q_i | k \rangle \langle l | Q_j | n \rangle \langle N' | F_i | N \rangle \langle N | F_j | N' \rangle \langle N' | \rho(0)_R | N' \rangle \\
 &\times \left(\frac{1}{i\sqrt{2\pi} (E_{N'} - E_N - \hbar\omega_{ln})} + \sqrt{\pi/2} \delta ((E_{N'} - E_N - \hbar\omega_{ln}) / \hbar) \right) \quad (41)
 \end{aligned}$$

For the real part of the nondiagonal coefficients, we have the following:

$$\text{Re}[\gamma_{12}] = \frac{W_{21} + W_{31} + W_{12} + W_{32}}{2} \quad (42)$$

$$\text{Re}[\gamma_{13}] = \frac{W_{31} + W_{21} + W_{13} + W_{23}}{2} \quad (43)$$

$$\operatorname{Re}[\gamma_{32}] = \frac{W_{13} + W_{23} + W_{21} + W_{32}}{2} \quad (44)$$

The imaginary part can be divided on two terms:

$$\begin{aligned} \operatorname{Im}[\Gamma_{\text{mkl}n}^+] &= -(1/\hbar)^2 \sum_{N'} |\langle 1; 0 | V | 2; N' \rangle|^2 \langle N' | \rho(0)_R | N' \rangle \frac{1}{\sqrt{2\pi} (E_{N'} - \hbar\omega_{21}) / \hbar} \\ &\quad - (1/\hbar)^2 \sum_N |\langle 1; N | V | 2; 0 \rangle|^2 \langle 0 | \rho(0)_R | 0 \rangle \frac{1}{\sqrt{2\pi} (-E_N - \hbar\omega_{21}) / \hbar} \\ &= -(1/\hbar)^2 \int d^3q |\langle 1; 0 | V | 2; N \rangle|^2 \exp[-\beta\hbar sq] \frac{1}{\sqrt{2\pi} (sq - \omega_{21})} \\ &\quad - (1/\hbar)^2 \int d^3q |\langle 1; N | V | 2; 0 \rangle|^2 \exp[-\beta E_0] \frac{1}{\sqrt{2\pi} (-sq - \omega_{21})} \end{aligned} \quad (45)$$

The first part contains the logarithmic divergence, but it is suppressed due to presence of term $\langle N' | \rho(0)_R | N' \rangle$ which is exponentially lower than $\langle 0 | \rho(0)_R | 0 \rangle$. The second part was calculated for our systems parameters, and it leads to 1,5 % percent reduction of frequency. This reduction is consistent with the more accurate calculation using adiabatic renormalization for superohmic bath [10].

Despite the another choice of approximating function fitting data in experimental work, we have time $T_2 = 0.50$ ns for double dot system [1] being close to $T_2^* = 0.18$ ns. We believe that the reason of this mismatch is Gaussian form of approximating function, and it underestimates the relaxation rate due to fast decrease.

3.4 Error estimates

In order to analyze the performance of the triple quantum dot system and its quality with respect to the fault-tolerant quantum computing criteria, one should estimate the error during one qubit oscillation time Δt . Consider the norm of the following deviation density operator σ

$$\sigma(t) = \rho(t) - \rho_{\text{ideal}}(t) \quad (46)$$

Where an “ideal” evolution is defined only by the Hamiltonian H_0 :

$$\rho_{\text{ideal}}(t) = e^{-iH_0 t/\hbar} \rho(0) e^{iH_0 t/\hbar} \quad (47)$$

And the error is defined by the measure of decoherence [11]

$$D(t) = \sup_{\rho(0)} (\|\rho(t) - \rho_{\text{id}}(t)\|) \quad (48)$$

To perform fault-tolerant quantum information processing, one needs to keep $D(\Delta t)$ below the fault-tolerant threshold. Following [12], in order to find the error due to the phase damping, one have to search for the maximum over the parameters in

$$\rho(0) = U(K |1\rangle \langle 1| + (1-K-L) |2\rangle \langle 2| + L |3\rangle \langle 3|)U^\dagger, \tag{49}$$

where $0 \leq K \leq 1$, $0 \leq L \leq 1 - K$ and U is an arbitrary 3×3 unitary matrix. This quantity should be compared with an error of double dot system

$$D_{\text{ph}}^{\text{db}}(t) = (1 - e^{-B^2(t)}) / 2 \tag{50}$$

After the numerical calculation, we found that the error due to phase damping in the triple quantum dot system can be well approximated with

$$D_{\text{ph}}^{\text{tr}}(t) = (1 - e^{-B_{12}^2(t)}) 2/3, \tag{51}$$

due to the relatively small difference between B_{12}^2 and B_{13}^2 .

The contribution of relaxation to the error of quantum qubit is calculated similarly. In the case of the qubit's subspace $|1\rangle \otimes |2\rangle$, one have to search the maximum of error over the parameter $0 \leq K \leq 1$ keeping $L = 0$. The largest deviation for this subspace can be well approximated with the following:

$$D_{12}^{\text{tr}}(t) = \frac{1 - e^{-\Gamma_{12}t}}{1 + e^{-E/kT}} \tag{52}$$

Here,

$$\Gamma_{12} = W_{12}^a + W_{12}^e + W_{23}^a + W_{23}^e. \tag{53}$$

The error of quantum qubit in the subspace $|1\rangle \otimes |3\rangle$ is

$$D_{13}^{\text{tr}}(t) = \frac{1 - e^{-\Gamma_{13}t}}{1 + e^{-E/kT}}, \tag{54}$$

with

$$\Gamma_{13} = W_{23}^a + W_{23}^e. \tag{55}$$

Finally, we can represent the error during one qubit oscillation time in the case of $\varepsilon_P = 0$ on the Fig. 4, and the error dependence from interdot distance on Fig. 5. The distance between two nearest extrema equals $\Delta L = \hbar s \pi / \varepsilon$ in the case of triple quantum dot with qubit subspace $|1\rangle \otimes |3\rangle$ and double dot system. The choice of subspace will lead to the different values of error rate.

4 Discussion

We analyzed decoherence rates of electron charge states in SiGe triple quantum dots. The decoherence was induced by anisotropic deformation interaction of electron with

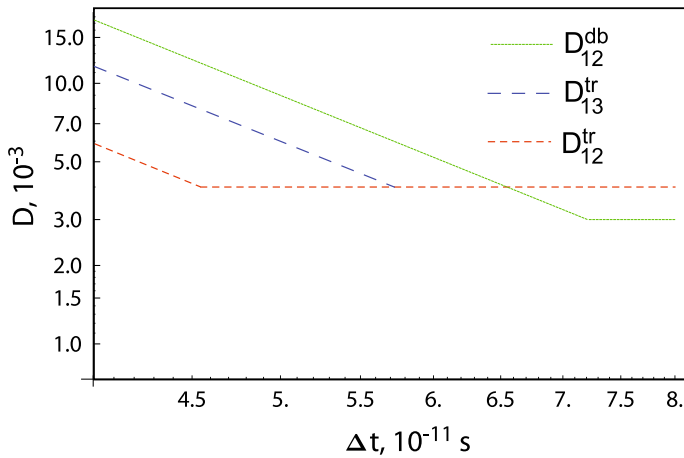


Fig. 4 Dependence of the error rate from qubit oscillation time, $L = 180 \text{ nm}$

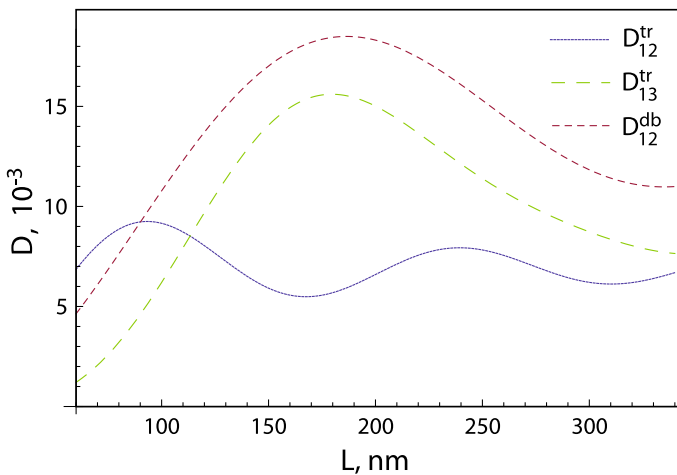


Fig. 5 Dependence of the error rate from interdot distance at $\Delta t = 4 * 10^{-11} \text{ s}$

acoustic phonons. Our results show that in wide range of parameters, triple quantum dot qubit architecture may have lower decoherence rate compared to double quantum dot qubits.

References

1. Shi, Z., Simmons, C., Ward, D., Prance, J., Koh, T.S., Gamble, J.K., Wu, X., Savage, D., Lagally, M., Friesen, M.: ArXiv preprint (2012). [arXiv:1208.0519](https://arxiv.org/abs/1208.0519)
2. Busl, M., Granger, G., Gaudreau, L., Sánchez, R., Kam, A., Pioro-Ladrière, M., Studenikin, S., Zawadzki, P., Wasilewski, Z., Sachrajda, A.: Bipolar spin blockade and coherent state superpositions in a triple quantum dot. *Nat. Nanotechnol.* **8**, 261–265 (2013)

3. Mehl, S., DiVincenzo, D.P.: Noise analysis of qubits implemented in triple quantum dot systems in a Davies master equation approach. *Phys. Rev. B* **87**, 195309 (2013)
4. Thalakulam, M., Simmons, C., Rosemeyer, B., Savage, D., Lagally, M., Friesen, M., Coppersmith, S., Eriksson, M.: Fast tunnel rates in Si/SiGe one-electron single and double quantum dots. *Appl. Phys. Lett.* **96**, 183104–183104 (2010)
5. Fischetti, M., Laux, S.: Band structure, deformation potentials, and carrier mobility in strained Si, Ge, and SiGe alloys. *J. Appl. Phys.* **80**, 2234–2252 (1996)
6. Friesen, M., Chutia, S., Tahan, C., Coppersmith, S.: Valley splitting theory of Si Ge/ Si/ Si Ge quantum wells. *Phys. Rev. B* **75**, 115318 (2007)
7. Palma, G.M., Suominen, K.A., Ekert, A.K.: Quantum computers and dissipation. *Proc. R. Soc. Lond. Ser. A Math. Phys. Eng. Sci.* **452**, 567–584 (1996)
8. Fedichkin, L., Fedorov, A.: Study of temperature dependence of electron–phonon relaxation and dephasing in semiconductor double-dot nanostructures. *IEEE Trans. Nanotechnol.* **4**, 65–70 (2005)
9. Blum, K.: *Density Matrix Theory and Applications*. Springer, Berlin (2012)
10. Leggett, A.J., Chakravarty, S., Dorsey, A., Fisher, M.P., Garg, A., Zwerger, W.: Dynamics of the dissipative two-state system. *Rev. Mod. Phys.* **59**, 1 (1987)
11. Fedichkin, L., Fedorov, A., Privman, V.: Measures of Decoherence. In: *Proc. SPIE 5105, Quantum Information and Computation*, pp. 243–254 (2003)
12. Fedichkin, L., Fedorov, A., Privman, V.: Additivity of decoherence measures for multiqubit quantum systems. *Phys. Lett. A* **328**, 87–93 (2004)